

COMPARATIVE STUDY ON COBALT AND NICKEL NPs FOR MWCNT GROWTH BY TCVD SYSTEM

SEPIDEH SADAT MADANI^a, KARIM ZARE^{a, b,*}, MAHMOOD
GHORANNEVISS^c AND MAJID MONAJJEMI^a

ABSTRACT. In this paper, cobalt and nickel NPs (nanoparticles) effect on carbon nanotubes growth by Thermal chemical vapor deposition (TCVD) is studied. The DC - sputtering system was used to prepare cobalt and nickel thin films on Si substrates. The produced layers were used as metal catalysts for growing carbon nanotubes (CNTs) from acetylene (C₂H₂) gas in the temperature range of 850°C to 1000°C with an interval of 50 C by Thermal Chemical Vapor Deposition (TCVD) technique. Energy Dispersive X-ray (EDX) measurements were used to investigate the elemental composition of the cobalt and nickel NPs deposited on the Si substrates. Also, Atomic Force Microscopy (AFM) was used to characterize the surface morphology of the Co and Ni nanoparticles on the Si substrates. The grown CNTs on the Co and Ni catalyst at different temperatures have been characterized by Raman spectroscopy, Field Emission Scanning Electron Microscopy (FESEM) and High Resolution Transmission Electron Microscopy (HRTEM). The results showed that the diameter of CNTs can be controlled by adjusting the growth temperature, and increasing the temperature leads to increasing the diameter of CNTs. It was found that there is a strong relation between diameter and yield of CNTs at different growth temperature with different catalysts (Co and Ni). Also, the grown CNTs at the temperature of the 850°C using Co catalyst among all of the samples (Co and Ni catalysts) have a minimum diameter and maximum yield.

Keywords: Carbon nanotubes, DC – sputtering, TCVD; Metal catalysts, FESEM, HRTEM

^a Department of Chemistry, Science and Research Branch, Islamic Azad University, Tehran, Iran

^b Department of Chemistry, Shahid Beheshti University, Tehran, Iran

^c Department of Physics, Science and Research Branch, Islamic Azad University, Tehran, Iran

* Corresponding author: prof.zare@gmail.com

INTRODUCTION

In the last decades, low dimensional carbon-based materials such as carbon nanotubes, polymer nanofibers, carbon nanotips, and graphene have attracted great attention due to their novel structures and extensive applications in the areas of nanoelectronic and nanophotonic devices, biology and medicine [1-7]. Three major methods have been developed to grow CNTs: arc discharge [8], laser ablation [9] and chemical vapor deposition (CVD) [10-12]. Among these methods CVD has attracted much attention owing to its advantages including lower cost, high yield, high purity and selective growth of CNTs. There are three main CVD techniques: 1- Thermal CVD (TCVD), 2- Plasma enhanced CVD (PECVD), and 3- Hot filament CVD (HFCVD) [11-13]. The growth of CNTs by CVD contains two steps: preparation of catalyst nanostructure layers and growth of CNTs on the layers. The chemical vapor deposition (CVD) provides a reliable approach to grow nanotubes on different substrates and is suitable for scaled growth of high purity multi-walled and single-walled carbon nanotubes. In addition, CVD operates at substantially lower temperature in comparison to laser ablation and arc discharge processes [14]. In this method, the characteristics of CNTs such as diameter distribution, surface density, morphology and crystallization are significantly affected by the synthesis parameters ranging from growth temperature, pressure, hydrocarbon source and type of substrate to the catalyst characteristics including its morphology, composition and the technique of catalyst preparation [15-21]. It is well known that the catalyst is indispensable for the growth of CNTs in CVD process. A variety of metal catalysts such as Au, Ag, Pt, Pd, Mn, Mo, Mg and Al have been developed for the growth of CNTs [22-26]. However, most of the widely used CNT production methods are based on the use of transition metal catalysts, including Fe, Co, Ni and their alloys [27].

There are several efforts related in the literature about growth time and/or temperature effect on the radius of the CNTs. The results achieved with acetylene (C_2H_2) and CVD technique shows that the diameters of the CNTs increase as the temperature increases [28-30]. It was generally thought that the increase in diameter is due to the extra concentric cylinders in multiwall CNTs. However, a recent study shows that the increase in the diameter is due to nanocrystalline carbon or glassy carbon sheath which expands exponentially with the time [30]. According to the literature, in nearly all CVD-based processes, the precursor gas is a mixture of hydrocarbon source and a diluting or carrier gas such as hydrogen, argon and ammonia.

Here we report a systematic study of the metal catalysts (Co and Ni) effect on the growth of CNTs using thermal CVD method. We have successfully achieved the tuning of the diameter distribution and yield of CNTs by varying the growth temperature using both (Co and Ni) catalysts.

RESULTS AND DISCUSSION

All the growth conditions except the temperature of the system were kept constant in order to investigate the effect of Co and Ni catalysts and temperature variation. Prior to carbon nanotube growth, Energy Dispersive X-ray (EDX) measurements were done to investigate the elemental composition of the cobalt (Figure 1a) and nickel (Figure 1b) catalysts deposited on Si substrates. Atomic Force Microscopy (AFM) in contact mode was used for analyzing the surface morphology of Co and Ni films deposited on Si substrates (Figure 2 (a-d)). AFM images have been obtained in a scanning area of $3\mu\text{m} \times 3\mu\text{m}$. As it is clear, the formation of catalyst particles with a relatively smooth surface can be observed. For the analysis of the uniformity of catalyst distribution along the substrate surface, it is helpful to calculate the roughness value. The average roughness values are 1.91 nm and 2.15 nm for Co and Ni samples, respectively. Root-Mean-Square (RMS) roughness of both samples was measured over the whole area and it was 2.44 nm and 3.27 nm for Co and Ni, respectively. The RMS roughness of a surface is similar to the roughness average, with the only difference being the mean squared absolute values of surface roughness profile.

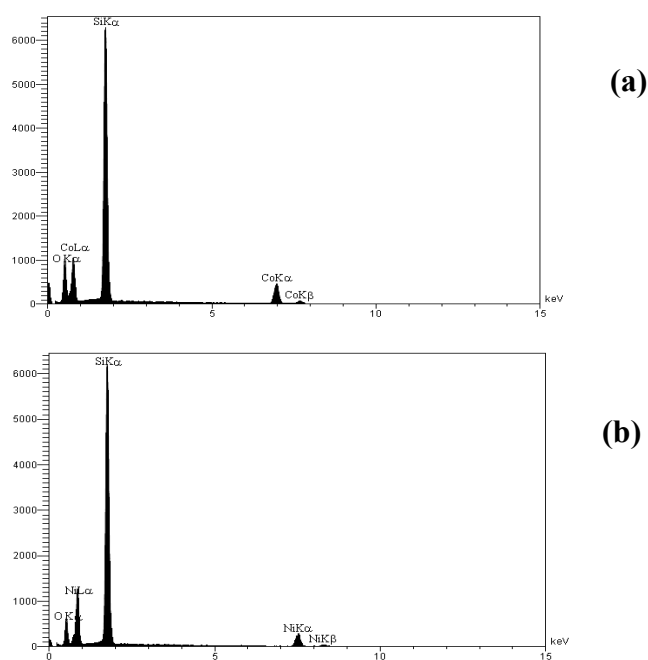


Figure 1. Energy Dispersive X-ray (EDX) measurements show the elemental composition of the (a) cobalt and (b) nickel nanoparticles deposited on Si substrates.

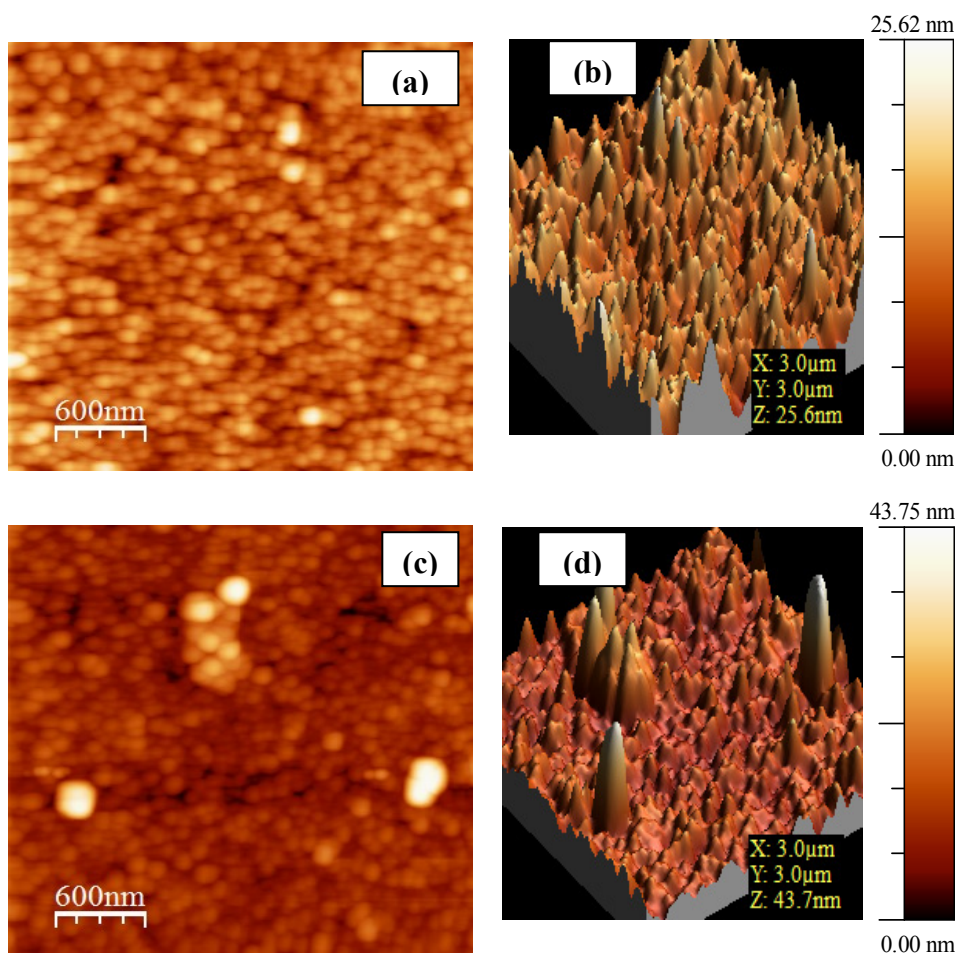


Figure 2. (a) 2D and (b) 3D AFM Images of Co film; (c) 2D and (d) 3D AFM Images of Ni film deposited on Si substrates.

Figure 3 (a-d) shows the FESEM images of CNTs grown on the cobalt nanocatalyst at different growth temperatures 850°C, 900°C, 950°C and 1000°C. In the presence of cobalt catalyst, as the growth temperature to 1000°C was increased, it was found that the diameter distribution of CNTs is raised, which implies that the diameter of grown CNTs increased and yield decreased. Figure 4 (a-d) shows the FESEM images of CNTs grown on the nickel nanocatalyst at different growth temperatures 850°C, 900°C, 950°C and 1000°C. A very small amount of CNTs was produced at 850°C on the Ni catalyst (Figure 4a). As the temperature increased to 900°C, the production of

CNTs has increased dramatically (Figure 4b). At 950°C compared to 900°C, a lower rate of CNTs was observed (Figure 4c). As can be seen in Fig. 4d, at 1000°C, nucleation was performed, but the growth has not taken place. Also, the grown CNTs at 850°C using Co catalyst among all of the samples (Co and Ni catalysts) have a minimum diameter and maximum yield.

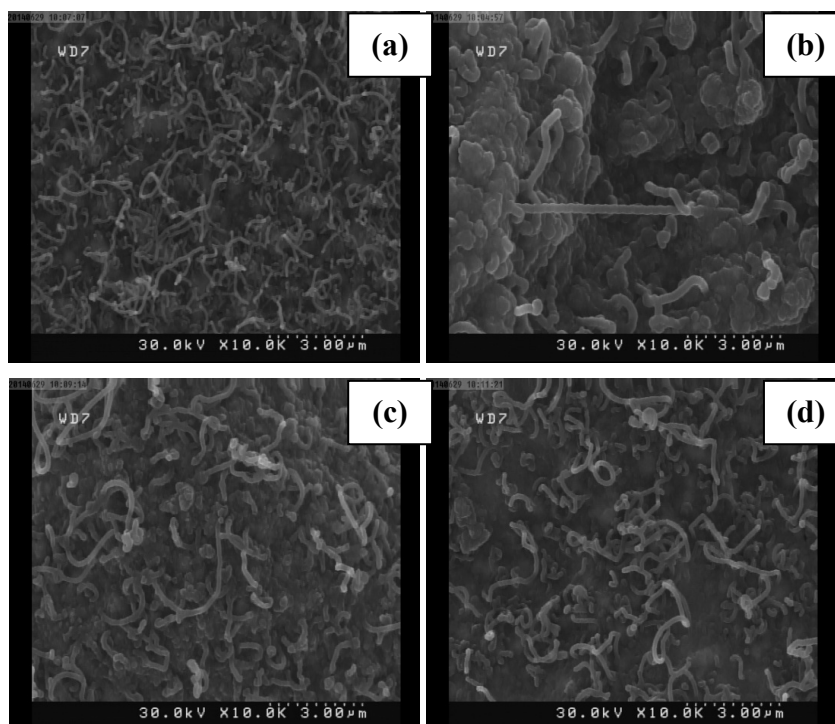


Figure 3. FESEM images of grown CNTs at different growth temperatures on the Co catalyst (a) 850 C, (b) 900 C, (c) 950 C, (d) 1000 C.

Since the quality and the structure of CNTs highly depends on the properties and the type of catalyst material being used, it is essential to study the catalysts. A key factor for controlling the diameter and the number of shells in a CNT is to gain control of the catalyst particle diameter, since they are the basis of the grown CNTs. Optimal growth requires a metal catalyst that exhibit sufficient carbon solubility, rapid carbon diffusion and limited carbide formation. It is important to mention that decomposition with common hydrocarbons, except CH_4 , is highly exothermic and can therefore dramatically increase the catalyst local temperature even if synthesis temperatures are low.

In general, the ability of transition metals to bond with carbon atoms increases with the number of unfilled d-orbitals. Metals with few d-vacancies such as Ni, Fe and Co exhibit finite carbon solubility. For transition metals, the affinity for carbon therefore increases from the right to the left of the periodic table [31-33]. Graphitic carbon will be allowed to form if the carbon concentration overcomes the solubility of carbon in the catalyst particle. For elements that do not form stable carbides (e.g. Cu, Ni, Co, Pb, Sn, Au, Ag, Zn, Cd, Pd, Pt) [34], the critical concentration for the segregation of graphitic carbon is therefore the solubility limit of carbon in the metal.

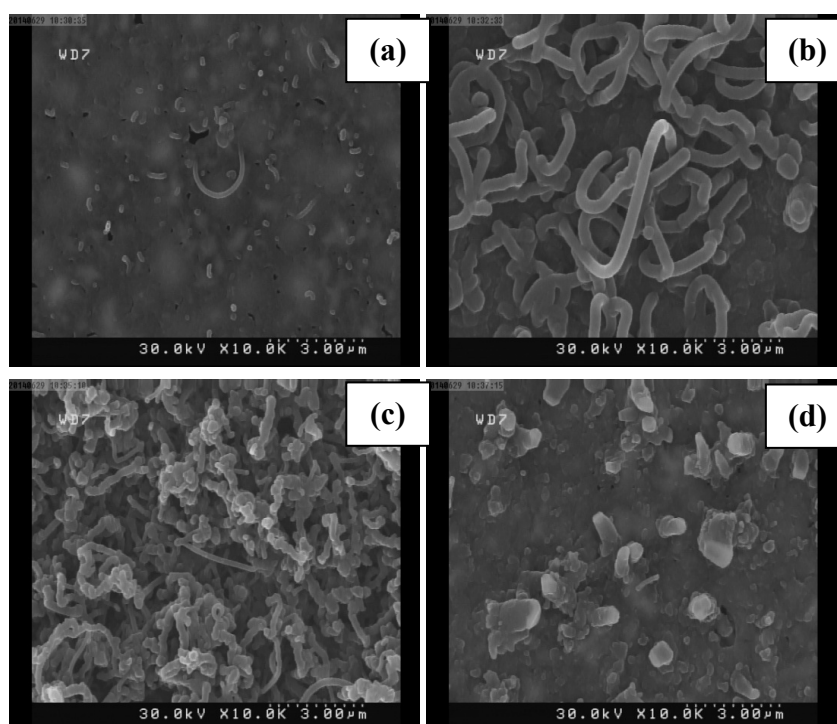


Figure 4. FESEM images of grown CNTs at different growth temperatures on the Ni catalyst (a) 850 C, (b) 900 C, (c) 950 C, (d) 1000 C.

The role of a catalyst is to accelerate a thermodynamically allowed chemical process (e.g. the decomposition of carbon containing molecules) by creating a transition state of lower energy [35]. The corresponding decrease of activation energy depends on the strength of the adsorbate–substrate bond which experimentally is reflected in the heat of adsorption. There is a general trend for the heats of adsorption to decrease from the left to the right of the

periodic table. This trend can be explained by the chemisorption model developed by Nørskov [36] stipulating that molecules adsorbing on transition metals preferentially interact with the d-states near the Fermi level that give rise to bonding and anti-bonding levels. The d-electron contribution to the bonding is therefore proportional to $(1 - f_d)$ where f_d is the degree of filling of the d-band.

When a molecule is adsorbed on a metal surface, the activation barrier for its dissociation is lowered. For instance, the activation barrier for the dissociation of acetylene was measured to be 1.4 eV on Ni (111) instead of 5.58 eV for self-decomposition [37]. If the surface bonds are too strong, the reaction intermediates will remain on the surface and block the adsorption of new reactant molecules. Forming adsorbate–substrate bonds of intermediate strength is an important property for a good catalyst.

It has long been recognized that the size and the surface structure of the catalyst can influence the catalytic activity. A catalytic reaction is defined as structure-sensitive if its conversion rate changes markedly as the size of the catalyst particles are changed. The reactivity of a metal surface is generally associated to both its geometric features and its electronic structure. Classically, the structure sensitivity of a catalytic reaction is associated with a modification of the population of reactive sites (terrace, steps, kinks, surface defects) with decreasing particle size [38].

According to Charles law of kinetic theory of gases [39], when temperature increases, then simultaneously volume of gas, kinetic energy of gas molecules and hence diffusion rate of gas molecules increase in the growth chamber. So when the growth temperature of CNTs increases, the decomposition rate of hydrocarbon in CVD chamber also increases and hence more carbon atoms make contact with catalyst particle and this is the main reason behind increasing the diameter of CNTs with increment in temperature. Also, as temperature increases the equilibrium between the decomposition of hydrocarbon and diffusion of carbon atoms in catalyst particle is also disturbed. So some carbon atoms are deposited on catalyst particle in the form of amorphous and these particles left from growth and hence yield of CNTs decreased.

A mechanism for the formation of carbon fibers on a catalyst particle was proposed by Baker and co-workers [40-42]. In their model, dissociation of carbon precursors on the catalyst surface was followed by diffusion of carbon into the metal catalyst particle. Once the catalyst was saturated with carbon, the carbon precipitated in the form of a fiber that continued to grow as more carbon dissociated and precipitated from the catalyst particle. The growth of carbon nanotubes is usually proposed to follow a similar mechanism. As with carbon spheres, the growing carbon fibers and tubes can also be covered with disordered graphitic flakes that are generated by gas phase carbon species that do not interact with the catalyst particle.

Histograms of diameter distribution of grown CNTs using Co and Ni catalysts, each fitted with a Gaussian curve, are demonstrated in Figure 5. According to these diagrams, the average diameter of the grown CNTs using Co and Ni catalysts is 114 nm and 295 nm, respectively. The average diameter of grown CNTs is greater than the average size of Co and Ni nanoparticles. In view of a direct relation between the nanocatalysts sizes with the diameters of grown CNTs, it can be suggested that the catalyst particles are agglomerated and resulted in greater particles during the process of CNT growth. It seems that such agglomeration is dramatically increased using Ni catalyst; consequently, the average diameter of grown CNTs using nickel catalyst is much larger than CNTs synthesized using cobalt catalyst.

Figure 6 shows the HRTEM image of the grown CNTs at a growth temperature of 850 °C using Co catalyst, which confirms that the morphologies seen in the FESEM images have tubular structure, i.e. they are multi-walled carbon nanotubes (MWCNTs).

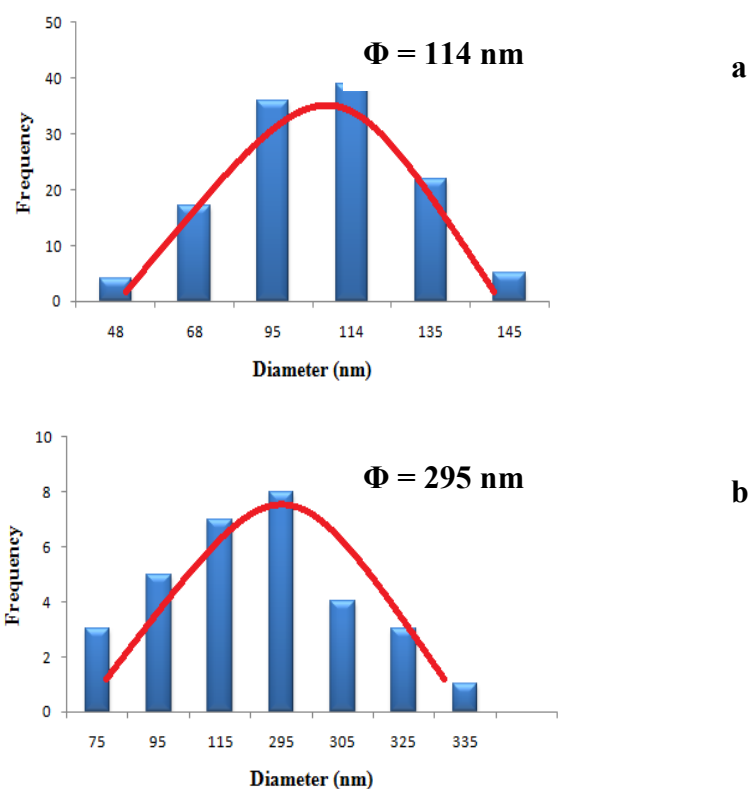


Figure 5. Histograms of diameter distribution of grown CNTs using (a) Co and (b) Ni catalysts. The diameter distributions are fitted with Gaussian curves.

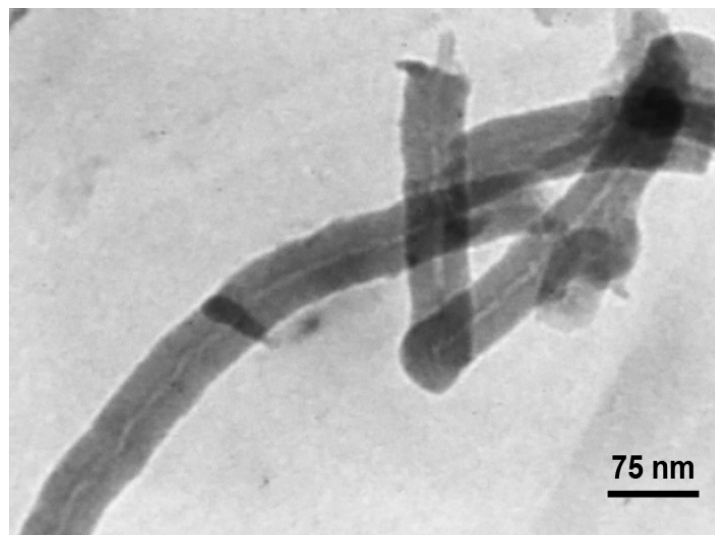


Figure 6. HRTEM image of the grown CNTs at growth temperature of 850°C using Co catalyst.

Raman spectroscopy is one of the most powerful tools for characterization of CNTs. The Raman spectrum of the produced CNTs on the cobalt catalyst at different growth temperatures is shown in Figure 7. The Raman band appearing in the 1500–1605 cm^{-1} region of the wave numbers is attributed to the G band (graphite band) and the one appearing in the 1250–1450 cm^{-1} spectral region is known as D band (disorder induced band). The G band is assigned to C–C vibration frequency of the carbon material with a sp^2 orbital structure and the D band is contributed to the disorder induced vibration of the C–C band [43]. In this work, there are two main peaks in the spectrum. The clear G band indicates the formation of graphitized MWCNTs and the D band indicates the existence of the disorder carbon, such as amorphous carbonaceous particles or defective graphite layers. Also, there is a peak in the region of the radial breathing mode (RBM), i.e. below 300 cm^{-1} of the spectrum. The RBM Raman features correspond to the atomic vibration of the C atoms in the radial direction. Raman spectra of CNTs grown on Co catalyst at the temperatures of 850°C and 950°C show RBM peak that it seems the presence of SWCNT in the cavity of MWCNT is responsible for the appearance of RBM in MWCNT as B. P. Singh et al. reported [44]. The peak intensity ratio I_G/I_D is recognized as a rough measure of sample quality because it is the relative response of graphite carbon to defective carbon.

The G'-band frequency is close to twice that of the D band and is found from 2500 to 2900 cm^{-1} . This is a second-order process from two zone boundary longitudinal optical (LO) phonons. The G' band is an intrinsic property of the nanotubes and graphite, and present even in defect-free nanotubes for which the D band is completely absent. The Raman spectrum of the produced CNTs on the nickel catalyst at different growth temperatures is shown in Figure 8. The ratios of the intensities of G and D peaks, I_G/I_D for produced CNTs by Co and Ni catalysts at different growth temperatures are presented in Table 1.

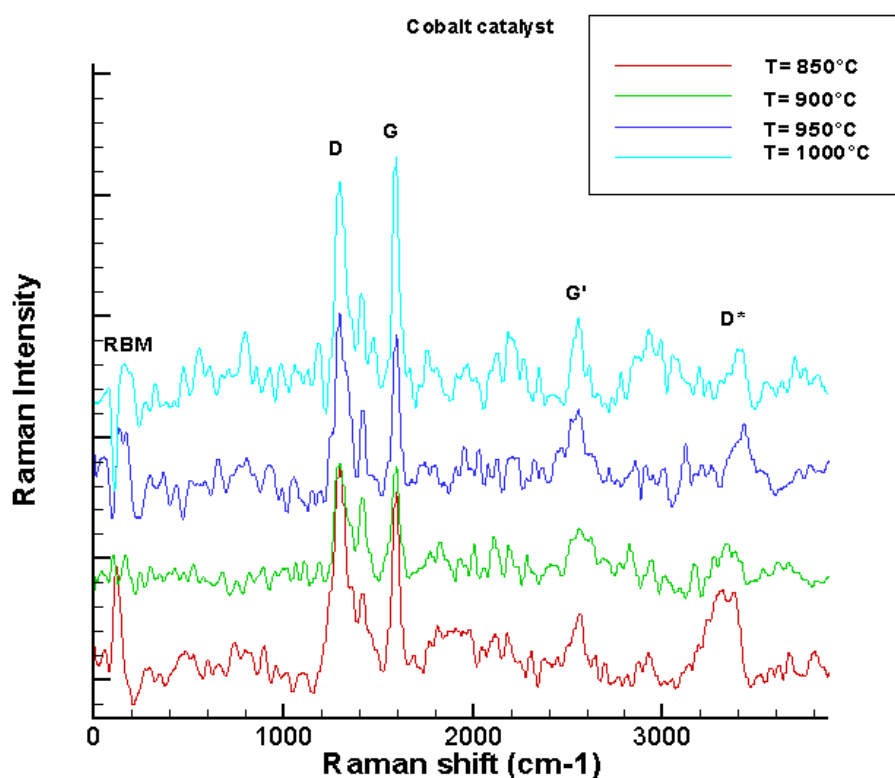


Figure 7. The Raman spectrum of the produced CNTs on the cobalt catalyst at different growth temperatures.

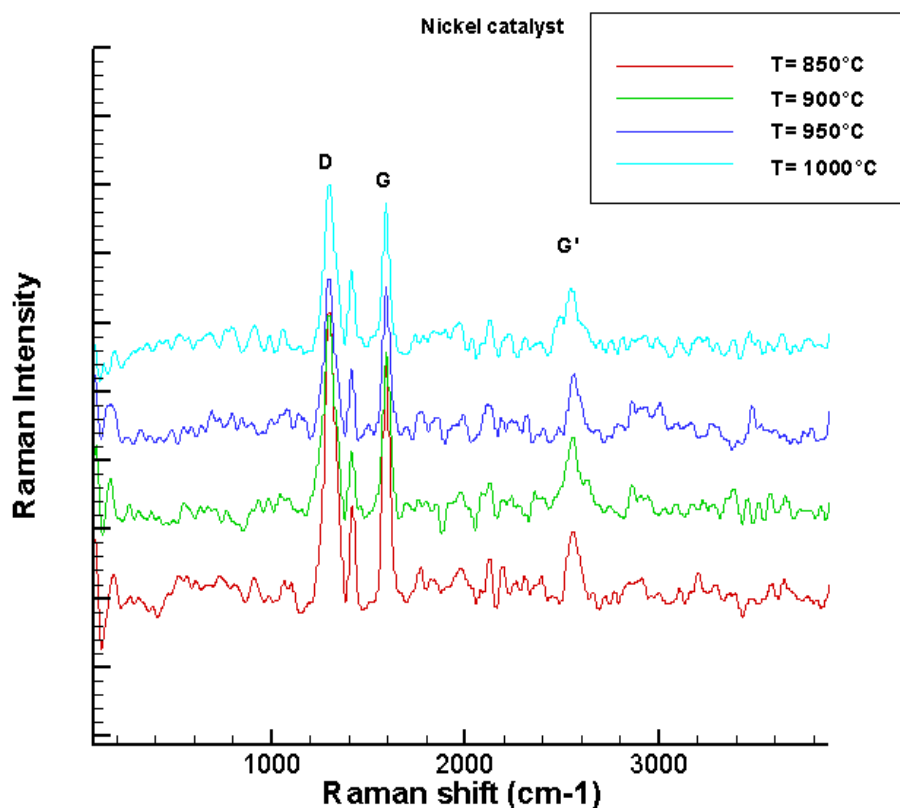


Figure 8. The Raman spectrum of the produced CNTs on the nickel catalyst at different growth temperatures.

Table 1. The ratios of the intensities of G and D peaks, I_G/I_D for produced CNTs by Co and Ni catalysts at different growth temperatures.

Catalyst	Growth temperature	G band (cm^{-1})	D band (cm^{-1})	I_G/I_D
Co	850°C	1594.56	1300.73	0.8982
Co	900°C	1595.69	1294.29	0.9563
Co	950°C	1594.56	1293.00	0.9155
Co	1000°C	1586.82	1293.00	1.0444
Ni	850°C	1591.77	1289.21	0.8049
Ni	900°C	1594.56	1300.73	0.8460
Ni	950°C	1586.82	1293.00	0.9411
Ni	1000°C	1584.40	1293.15	0.8737

Here, the ratio of I_G/I_D is greater than one for the grown CNTs by Co catalyst at a growth temperature of 1000°C indicates that the grown CNTs have good crystalline graphite structure while from FESEM results, it was found that at this temperature the diameter of CNTs is raised and their yield decreased.

CONCLUSIONS

In this paper, the growth of carbon nanotubes over Co and Ni nanoparticles in a temperature range of 850°C-1000°C was studied. Cobalt and nickel nanoparticles were deposited onto the p-type Si (400) wafers by planar DC-sputtering system. The results showed that the diameter of CNTs can be controlled by adjusting the growth temperature, and increasing the temperature leads to increasing the diameter of CNTs. Also, the ratio of I_G/I_D is greater than one for the grown CNTs using Co catalyst at a growth temperature of 1000°C indicates that the grown CNTs have good crystalline graphite structure. FESEM results showed that the grown CNTs at the temperature of the 850°C using Co catalyst among all of the samples (Co and Ni nanoparticles) have a minimum diameter and maximum yield while a very small amount of CNTs produced at the same temperature using Ni catalyst. For transition metals, the affinity for carbon increases from the right to the left of the periodic table. So, the affinity of cobalt for carbon is greater than the affinity of nickel.

On the role of CNT catalysts, it is worth mentioning that transition metals are proven to be efficient catalysts, not only in CVD but also in arc-discharge and laser-vaporization methods. Therefore, it is likely that these apparently different methods might inherit a common growth mechanism of the CNT, which is not yet clear. Hence this is an open field of research to correlate different CNT techniques in terms of the catalyst's role in entirely different temperature and pressure range.

EXPERIMENTAL SECTION

In the present investigation, p-type Si (400) wafers with size of 1cm × 1cm were used as substrates. The wafers were cleaned by ultrasonic method in acetone and ethanol solutions to remove potential residual contaminants prior to deposition. The samples were introduced into the planar DC-sputtering system and then pumped down to a base pressure of 4×10^{-1} Pa. A cobalt plate was used as a cathode and was placed in parallel with the oven which was grounded. The distance between the cathode and anode was about 1 cm.

Argon was introduced into the chamber with a flow of 200 Standard Centimeter Cubic per Minutes (sccm). The cobalt NPs were sputtered on Si substrates when the substrate temperature gradually increased up to 100°C. Deposition time for cobalt sputtering was 30 minutes. This procedure with same conditions was repeated for nickel samples.

The Thermal Chemical Vapor Deposition (TCVD) system in the experiment (Figure 9) was an electric furnace composed of a horizontal quartz glass tube with an internal diameter of 7.5 cm and a length of 80 cm which was operated at atmospheric pressure.

Argon gas with a flow rate of 200 sccm was supplied into the CVD reactor to prevent the oxidation of catalytic metal while raising the temperature to 750°C. The samples were placed in the chamber and the temperature increased to 850°C. After that, Ar flow was switched off. For CNT growth, we used C₂H₂ / NH₃ at 35 / 60 sccm for 15 minutes. The growth was terminated by turning off C₂H₂ / NH₃ flow and the samples were allowed to cool down to room temperature under Ar gas flow. Same experiments were repeated with growth temperature as 850°C, 900°C, 950°C and 1000°C while keeping other growth parameters constant.

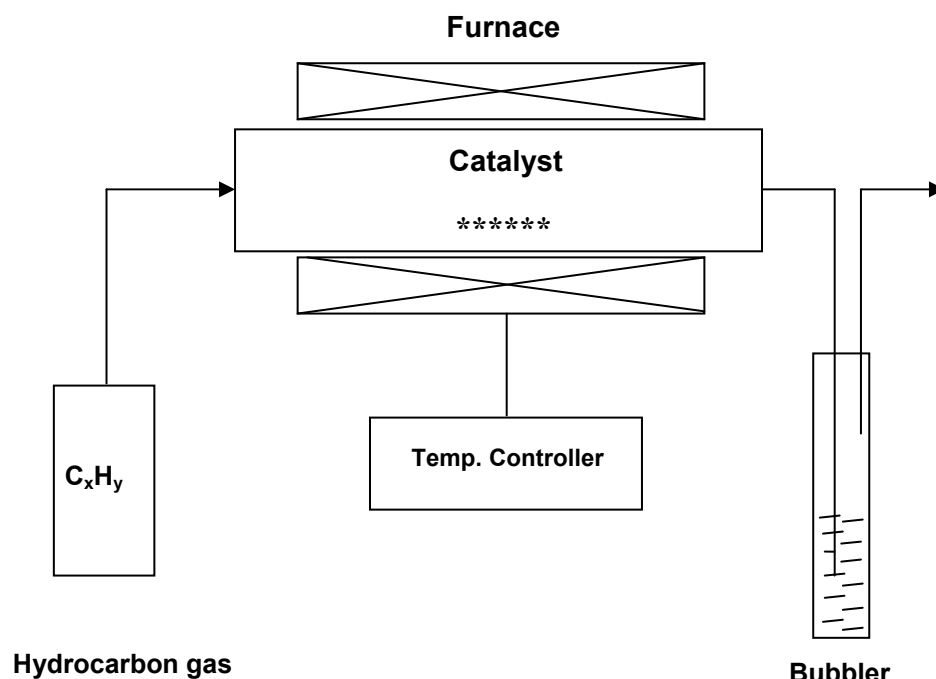


Figure 9. Schematic diagram of TCVD system of nanotube synthesis.

ACKNOWLEDGMENTS

The authors would like to express their thanks to Shahram Solaymani (PhD candidate, Young researchers and Elite club, Islamic Azad University, Kermanshah Branch, Iran) and Dr. Zahra Khalaj (Physics department, Shahre-Qods branch, Islamic Azad University, Tehran, Iran) for their help and cooperation.

REFERENCES

- [1]. Z.L. Tsakadze, K. Ostrikov, C.H. Sow, S.G. Mhaisalkar, Y.C. Boey, *Journal of Nanoscience and Nanotechnology*, 2010, 10, 6575.
- [2]. B. Liu, W. Ren, L. Gao, S. Li, S. Pei, C. Liu, C. Jiang, H.-M. Cheng, *Journal of the American Chemical Society*, 2009, 131, 2082.
- [3]. H. Yu, D. Liao, M.B. Johnston, B. Li, *ACS Nano*, 2011, 5, 2020.
- [4]. B.B. Wang, Q.J. Cheng, X.X. Zhong, Y.Q. Wang, Y.A. Chen, K. Ostrikov, *Journal of Applied Physics*, 2012, 111, 044317.
- [5]. D.H. Seo, S. Kumar, K. Ostrikov, *Carbon*, 2011, 49, 4331.
- [6]. A. Bianco, K. Kostarelos, M. Prato, *Current Opinion in Chemical Biology*, 2005, 9, 674.
- [7]. C.D. Modi, S.J. Patel, A.B. Desai, R.S.R. Murthy, *Journal of Applied Pharmaceutical Science*, 2011, 1, 103.
- [8]. C. Journet, W.K. Maser, P. Bernier, P.A. Loiseau, M.L. de la Chapelle, S. Lefrant, P. Deniard, R. Lee, J.E. Fischer, *Nature*, 1997, 388, 756.
- [9]. A. Thess, R. Lee, P. Nikolaev, H. Dai, P. Petit, J. Robert, C. Xu, Y.H. Lee, S.G. Kim, A.G. Rinzler, D.T. Colbert, G.E. Scuseria, D. Toma'nek, J.E. Fischer, R.E. Smalley, *Science*, 1996, 273, 483.
- [10]. H. Dai, *Surf. Sci.*, 2002, 500, 218.
- [11]. M. Meyyappan, L. Delzeit, A. Cassell, D. Hash, *Plasma Sources Sci. Technol.*, 2003, 12, 205.
- [12]. J.M. Bonard, *Thin Solid Films*, 2006, 501, 8.
- [13]. S. Porro, S. Musso, M. Giorcelli, A. Chiodoni, A. Tagliaferro, *Physica E*, 2007, 37, 16.
- [14]. A.M. Cassell, J.A. Raymakers, J. Kong, H. Dai, *J. Phys. Chem. B.*, 1999, 103, 6484.
- [15]. Y. Chen, D. Ciuparu, S. Lim, Y. Yang, G.L. Haller, L. Pfefferle, *J. Catal.*, 2004, 225, 453.
- [16]. L. Zheng, X. Liao, Y. T. Zhu, *Mater. Lett.*, 2006, 60, 1968.
- [17]. C. Dang, T. Wang, *Appl. Surf. Sci.*, 2006, 253, 904.
- [18]. K. Hernadi, A. Fonseca, J.B. Nagy, A. Siska, I. Kiricsi, *Appl. Catal. A: Gen.*, 2000, 199, 245.

- [19]. O.A. Nerushev, R.E. Morjan, D.I. Ostrovskii, M., Jonsson, M. Sveningsson, F. Rohmund, E. E. B. Campbell, *Physica B*, 2002, 323, 51.
- [20]. P. Sampedro-Tejedor, A. Maroto-Valiente, D. M. Nevskaya, V. Muñoz, I. Rodríguez-Ramos, A. Guerrero-Ruiz, *Diamond Relat. Mater.*, 2007, 16, 542.
- [21]. A.C. Dupuis, *Prog. Mater. Sci.*, 2005, 50, 929.
- [22]. W. Zhou, Z. Han, J. Wang, Y. Zhang, Z. Jin, X. Sun, Y. Zhang, C. Yan, Y. Li, *Nano Lett.*, 2006, 6, 2987.
- [23]. S. Bhaviripudi, E. Mile, S.A. Steiner III, A.T. Zare, M.S. Dresselhaus, A.M. Belcher, J. Kong, *J. Am. Chem. Soc.*, 2007, 129, 1516.
- [24]. D. Takagi, Y. Homma, H. Hibino, S. Suzuki, Y. Kobayashi, *Nano Lett.*, 2006, 6, 2642.
- [25]. D. Yuan, L. Ding, H. Chu, Y. Feng, T.P. McNicholas, J. Liu, *Nano Lett.*, 2008, 8, 2576.
- [26]. B. Liu, W. Ren, L. Gao, S. Li, Q. Liu, C. Jiang, H.-M. Cheng, *J. Phys. Chem. C*, 2008, 112, 19231.
- [27]. G. Hong, Y. Chen, P. Li, J. Zhang, *Carbon*, 2012, 50, 2067.
- [28]. C.J. Lee, J. Park, Y. Huh, J. Yong Lee, *Chem. Phys. Lett.*, 2001, 343, 33.
- [29]. S. Bandow, S. Asaka, Y. Saito, A.M. Rao, L. Grigorian, E. Richter, P.C. Eklund, *Phys. Rev. Lett.*, 1998, 80, 3779.
- [30]. F.H. Kaatz, M.P. Siegal, D.L. Overmyer, P.P. Provencio, D.R. Tallant, *Appl. Phys. Lett.*, 2006, 89, 241915.
- [31]. M. Hoch, "Phase stability of carbon in FCC and BCC metals", *Calphad*, 1988, 83.
- [32]. O.V. Yazyev, A. Pasquarello, *Phys. Rev. Lett.*, 2008, 100, 156102.
- [33]. R. Yang, P. Goethel, J. Schwartz, C. Lund, *J. Catal.*, 1990, 122, 206.
- [34]. G. Samsonov, *Powder Metall. Met. Ceram.*, 1965, 4, 75.
- [35]. G.A. Somorjai, "Introduction to surface chemistry and catalysis", Wiley, New York, 1994.
- [36]. J. Nørskov, *Phys. Rev. B*, 1982, 26, 2875.
- [37]. S. Hofmann, G. Csanyi, A.C. Ferrari, M.C. Payne, J. Robertson, *Phys. Rev. Lett.*, 2005, 95, 36101.
- [38]. V. Jourdain, C. Bichara, *Carbon*, 2013, 58, 2.
- [39]. N. Tripathi, P. Mishra, Harsh, S.S. Islam, "Effect of Growth Temperature on the Diameter Distribution and Yield of Carbon Nanotubes", *Physics of Semiconductor Devices, Environmental Science and Engineering*, Springer, 2014, 645.
- [40]. B. RTK, P.S. Harris, "Formation of filamentous carbon in chemistry and physics of carbon", *Chemistry and Physics of Carbon*, Marcel Dekker, New York, 1978, 83.
- [41]. B. RTK, *Carbon*, 1989, 27, 315.
- [42]. A. Oberlin, M. Endo, T. Koyama, *J. Cryst. Growth*, 1976, 32, 335.
- [43]. M.S. Dresselhaus, G. Dresselhaus, A. Jorio, A.G. Souza Filho, R. Saito, *Carbon*, 2002, 40, 2043.
- [44]. R. Gupta, B.P. Singh, V.N. Singh, T.K. Gupta, R.B. Mathur, *Carbon*, 2014, 66, 724.